Lewy-MSA hybrid fold drives distinct neuronal α-synuclein pathology

Masahiro Enomoto[1], Ivan Martinez-Valbuena[2], Shelley L. Forrest[2], Xiaoxiao Xu[3] Renato P. Munhoz[4,5], Jun Li[2], Ekaterina Rogaeva[2], Anthony E. Lang[2,4], Gabor G. Kovacs[2,4,5,6,7]

[1] Princess Margaret Cancer Centre, University Health Network, Toronto, ON, M5G 1L7, Canada
[2]Tanz Centre for Research in Neurodegenerative Diseases, University of Toronto, Toronto, Canada
[3]Department of Medical Biophysics, University of Toronto, Toronto, Canada
[4]Edmond J. Safra Program in Parkinson's Disease and the Morton and Gloria Shulman Movement Disorders Clinic, Toronto Western Hospital, M5T 2S8, Toronto, Ontario, Canada
[5]Krembil Brain Institute, University Health Network, Toronto, M5T 0S8, Ontario, Canada
[6]Department of Laboratory Medicine and Pathobiology, University of Toronto, Toronto, Canada;
[7]Laboratory Medicine Program, University Health Network, Toronto, Canada

Suppl-Table 1. Summary of cases examined for biochemistry and seeding.

Case	Age	Sex	Aβ Thal phase	NFT Braak stage	CAA: Cerebral amyloid angiopathy	Lewy Body Braak Stage	TDP-43 pathology (LATE-NC)	Other
atypical MSA	68	M	-	Stage II	-	-	-	Argyrophilic grain disease
MSA-P	64	F	Phase 5	Stage II	Aβ-positive Type 1	-	-	-
LBD	60	M	Phase 1	Stage III	-	6	-	Argyrophilic grain disease
Control	74	m	-	-	-	-	-	-

Suppl-Table 2. Genomic analysis

Genomic DNA for the atypical MSA cases was isolated from brain using a QIAGEN kit. The entire open reading frame of the *SNCA* gene was Sanger sequenced using the primers shown the table. Gene dosage of the *SNCA* gene region on chromosome 4 was determined by inspecting the B allele frequency and LogR Ratio plots (Figure) of Neurobooster array data of 155 SNPs in genomestudio (Illumina Inc., CA).
Table. Sequences of primers used in Sanger sequencing of *SNCA*.

SNCA_exon1_F	TTTGTCCAATGGTTAAATGAGTG
SNCA_exon1_R	CCTTTTTGACAAGCAATGATG
SNCA_exon2_F	CCTCCTGTTAGCTGGGCTTT
SNCA_exon2_R	GCTCAGTGATTGTTTTACAATTTCA
SNCA_exon3_F	TGGCTTTTGTTTCTTCTGACC
SNCA_exon3_R	GTAGCCGTTCCCCACAGTAA
SNCA_exon4_F	CGGAGGCATTGTGGAGTTTA
SNCA_exon4_R	TGCAAGTTGTCCACGTAATGA
SNCA_exon5_F	GCAGAATATTTGCAAAAACATTGAT
SNCA_exon5_R	GAAGCACCGAAATGCTGAGT

Suppl-Table 3. Statistics for cryo-EM data acquisition and atomic model building.

	Lewy-MSA temporal cortex (EMD-47820, PDB 9E9X)	**Lewy-MSA frontal cortex (EMD-70295, PDB 9OBP)**
Data acquisition		
Microscope	Titan Krios G3	Titan Krios G3
Detector	Falcon 4i	Falcon 4i
Energy filter slit (eV)	-	10
Magnification	75,000	75,000
Voltage (kV)	300	300
Exposure rate (e/pix/s)	6.8	7.5
Electron dose (e/Å^2)	41	45
Defocus range (μm)	1.3-3.0	0.8-2.0
Pixel size (Å)	1.03	0.93
Map refinement		
Symmetry imposed	C1	C1
Initial particle images (No.)	155,610	114,083
Final particle images (No.)	47,227	67,027
Map resolution (Å)	3.2	2.5
FSC threshold	0.143	0.143
Helical twist (°)	-1.2857	-1.38000
Helical rise (Å)	4.68955	4.75000
Model refinement		
Model resolution (Å)	3.2	2.7
FSC threshold	0.5	0.5
Map sharpening *B* factor (Å^2)	-53.1206	-38.3614
Model composition		
Non-hydrogen atoms	3,223	5,315
Protein residues	466	750
Ligands	0	0
B factors (Å^2)		
Protein	33.55	35.00
R.m.s. deviation		
Bond lengths (Å)	0.005	0.004
Bond angles (°)	0.938	0.948
Validation		
MolProbity score	2.15	1.85
Clashscore	13.93	13.05
Poor rotamers (%)	0.00	0.00
Ramachandran plot		
Favored (%)	91.55	96.58
Allowed (%)	8.45	3.42
Disallowed (%)	0	0

DETAILED NEUROPATHOLOGY

Neuropathology examination showed mild loss of neurons in the frontal (suppl-**Suppl-Fig 1f**), motor (**Suppl-Fig 1g**), and temporal cortex. The caudate nucleus was preserved (**Suppl-Fig 1h**), but the putamen showed severe gliosis (**Suppl-Fig 1i**), while the globus pallidus did not show neuronal loss (**Suppl-Fig 1j**). The left-side hippocampus had a normal morphology without mentionable gliosis (**Suppl-Fig 1k**). The right-side hippocampus was not available for histology (only frozen sample). Eosinophilic neuronal cytoplasmic inclusions were detected mostly in the granule cells of the dentate gyrus (**Suppl-Fig 1l**). The amygdala showed severe gliosis and eosinophilic inclusion bodies in neurons (**Suppl-Fig 1m**) with more prominent changes in the right side. Ballooned neurons were noted in the amygdala. The substantia nigra (**Suppl-Fig 1n**) and pontine base showed gliosis and patchy Purkinje cell loss was noted in the cerebellum (**Suppl-Fig 1o**). Brainstem type Lewy bodies were not seen. Immunostaining for α-synuclein showed neuronal cytoplasmic inclusions and threads of the frontal (**Suppl-Fig 1p**) and temporal cortex. The number of neuronal inclusions in the frontal cortex was less compared to the hippocampus and amygdala and less were seen in Hematoxylin and eosin staining. This was associated with a lower number of Papp-Lantos bodies in the white matter (**Suppl-Fig 1q**) of the frontal and temporal but more in the motor area. Prominent α-synuclein immunoreactive Papp-Lantos bodies were seen in the internal capsule (**Suppl-Fig 1r**), subinsular peri-putamen white matter and putamen, and less in the cerebral peduncles, pontine base, medulla oblongata, and the cerebellar white matter (**Suppl-Fig 1s**). Frequent cytoplasmic and nuclear neuronal inclusions and threads were noted in the putamen and less in brainstem nuclei. The amygdala exhibited many large spherical neuronal α-synuclein inclusions (**Suppl-Fig 1t**). Immunostaining for α-synuclein, p62 and AT8 also showed prominent pathologies in the hippocampus (**Suppl-Fig 1u-w**). Many α-synuclein positive neuronal inclusions were seen in the CA1 subregion and low amounts of Papp-Lantos bodies were seen in the hippocampal white matter (**Suppl-Fig 1x, y**). Round, Pick-body-like, and ring-like neuronal cytoplasmic α-synuclein positive inclusions predominated in granule cells of the dentate gyrus (**Suppl-Fig 1z1**); many of these showed p62-immunoreactivity (**Suppl-Fig 1z2**) and were Gallyas-Braak silver positive. Both neuronal and oligodendroglial α-synuclein inclusions were detected also using antibodies 5G4 (**Suppl-Fig 1**), MJFR1, and phosphoSyn129 (**Suppl-Fig 2**). In addition, a few granule cells showed fine granular AT8- (**Suppl-Fig 1z3**) but not phosphorylated TDP-43-immunoreactivity (**Suppl-Fig 1z4**). This was accompanied by oligodendrocytic coiled bodies in the hippocampus and amygdala white matter, granular/fuzzy astrocytes in the amygdala, and argyrophilic 4-repeat tau- and p62-immunopositive dendritic grains. Moderate numbers of neurofibrillary tangles and neuropil threads were observed in the entorhinal cortex.

Suppl-Fig.1. Brain MRI and histopathology (*next page*).

FLAIR (**a, b**) and T2 weighted (**c-e**) images showing bilateral putamen atrophy and hyperintensity surrounding the putamen (**a-d**) and medial temporal lobe and amygdala atrophy (**e**; indicated by white arrow; right > left). Hematoxylin and eosin and Luxol staining of the frontal (**f**), motor (**g**) cortex, caudate nucleus (**h**), putamen (**i**), globus pallidus (**j**), hippocampus (**k**), dentate gyrus (**l;** arrows indicate eosinophilic inclusions), amygdala (**m**), substantia nigra (**n**), and cerebellum (**o**). Immunostaining α-synuclein, clone 5G4 (**p-u, x, y, z_1**), p62 (**v, z_2**), phosphorylated tau (**w, z_3**) and phosphorylated TDP-43 (**z_4**) of the frontal cortex (**p**) and white matter (**q**), internal capsule (**r**), cerebellum white matter (**s**), amygdala (**t**), hippocampus (**u-w**), CA1 subregion (**x**), hippocampal white matter (**y**), and granule cell layer of the dentate gyrus (**z_{1-4}**). Bar in (**e**) represents 250 μm for **f-j**, **m**, **n**, **r-t**; 150 μm for **o**, **x**; 100 μm for **p**, **q**; 500 μm for **k**, **u**, **v**, **w**; 50 μm for **l**; 200 μm for **y**; 35 μm for **z_{1-4}**.

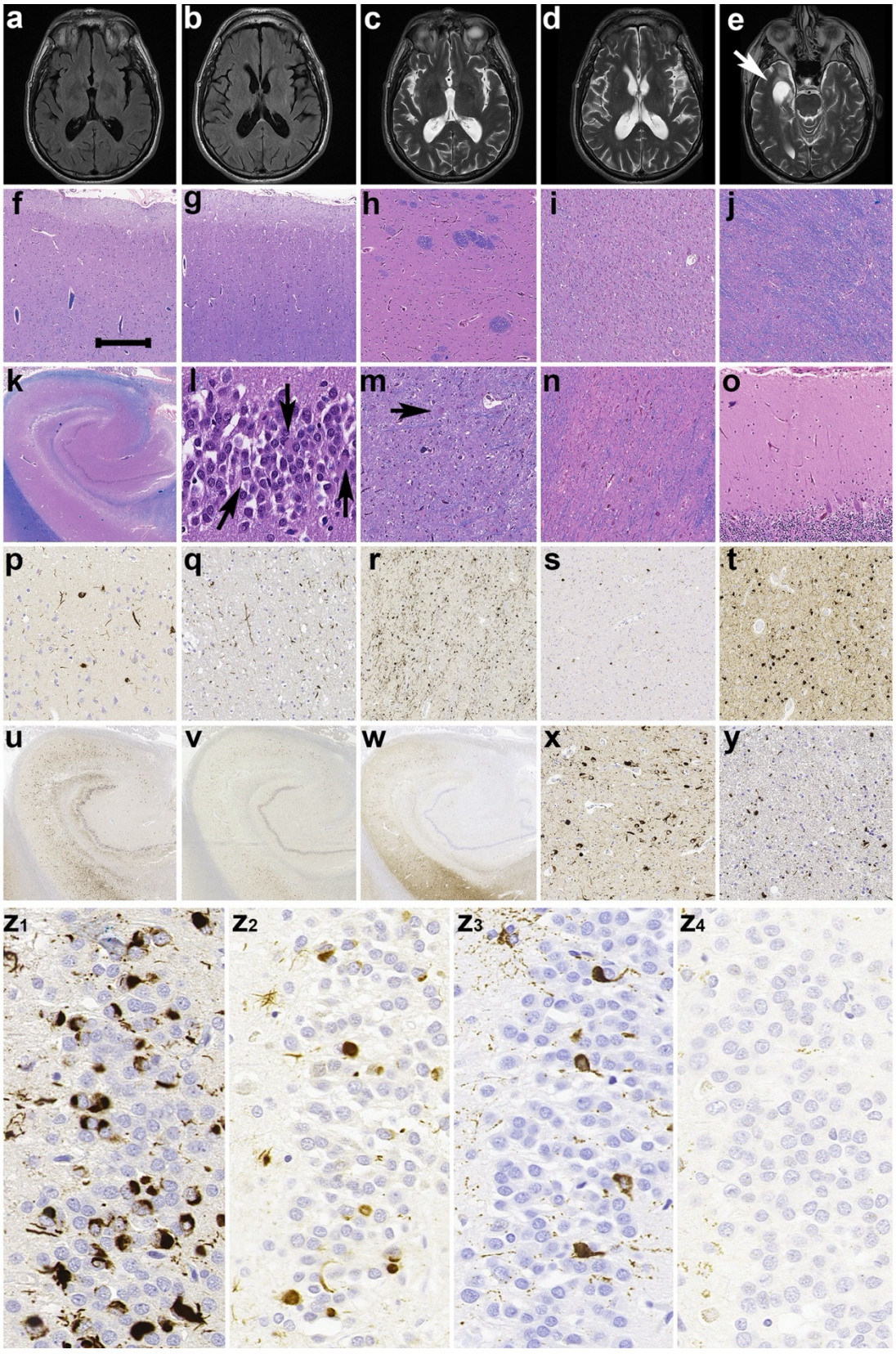
a
b
c
d
e
f
g
h
i
j
k
l
m
n
o
p
q
r
s
t
u
v
w
x
y
z1
z2
z3
z4

Suppl-Fig.2. Immunostaining for further anti-α-synuclein antibodies.
Using MJFR1 clone, 1:10,0000 dilution, ref: ab138501, Abcam; **a-c**) and the phosphorylated at Serine 129 α-synuclein (EP1536Y clone, 1:500 dilution, ref:51253, Abcam; **d-f**) reveals similar pathology as seen using 5G4 antibody (see Suppl. Fig.1): neuronal inclusions in the hippocampus dentate gyrus (**a, d**) and amygdala (**b, e**), and oligodendroglial and neuronal in the striatum (**c, f**). Bar in (**a**) represents 60 μm for all images.

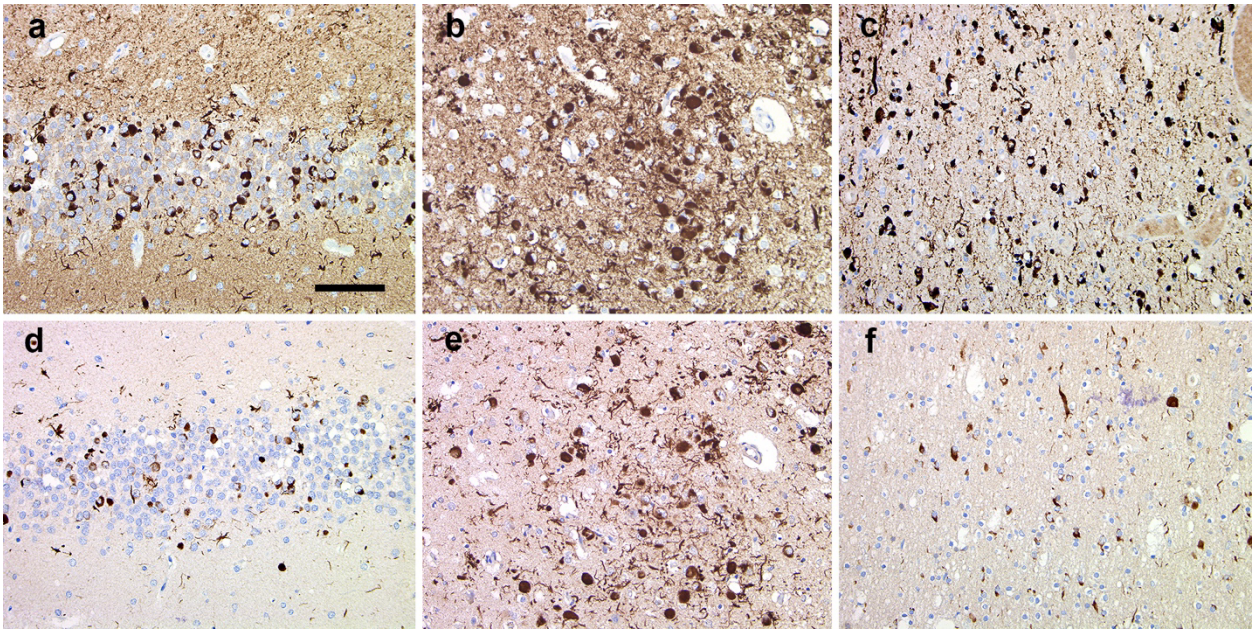

Suppl-Fig.3. **Conformational Stability of α-Synuclein Aggregates in Detergent-Soluble Brain Extracts from MSA and LBD Patients.** Representative α-synuclein immunoblots (Syn-1 clone) and corresponding denaturation curves from the conformational stability assay (CSA) are shown for detergent-soluble extracts from the cerebellum of an MSA patient (**a**), cerebellum (**b**) and temporal cortex (**c**) of an atypical MSA patient, and temporal cortex of an LBD patient (**d**). GdnCl: guanidine hydrochloride; M: molar.

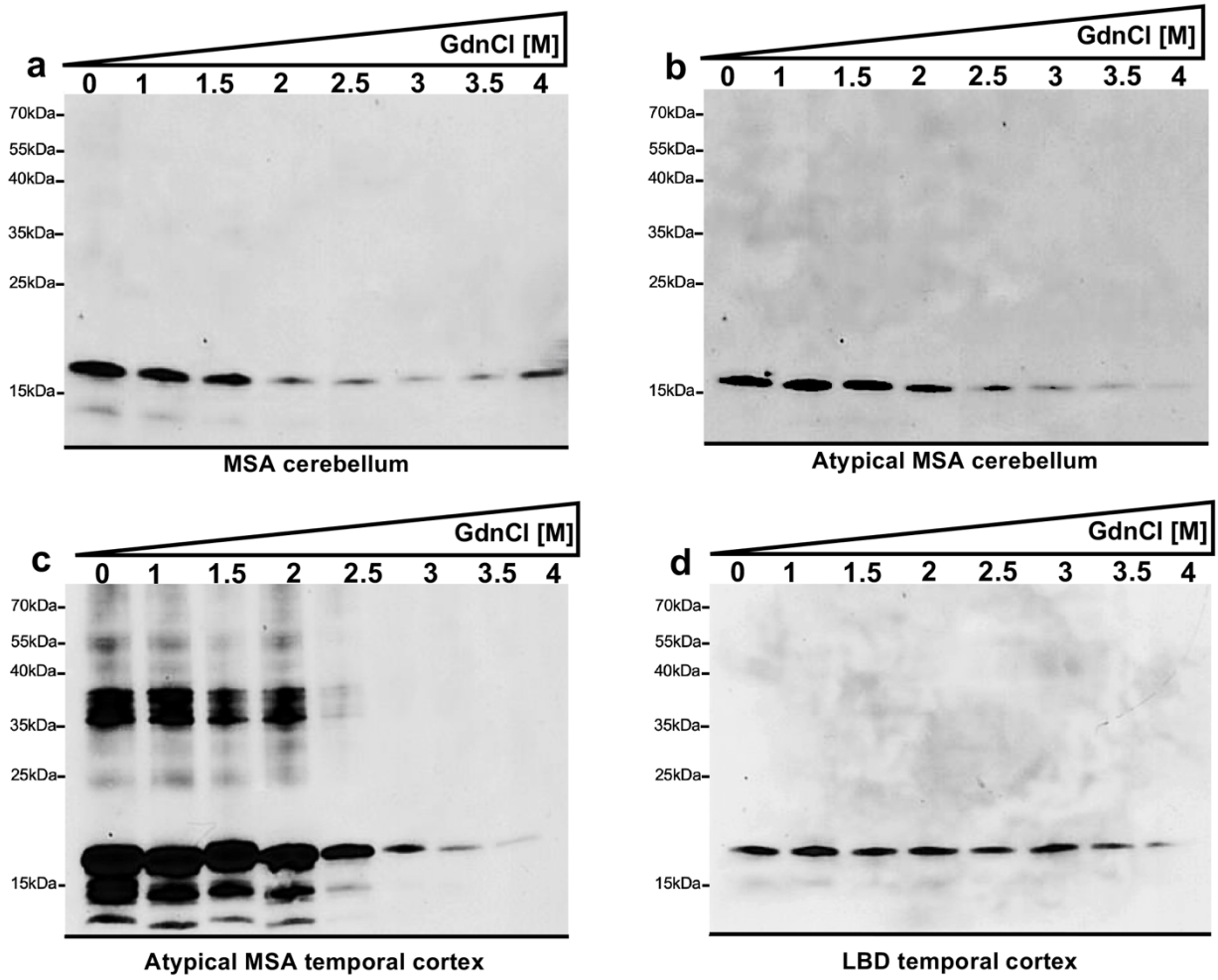

Suppl-Fig. 4. Cryo-EM images of the samples from the temporal cortex and the frontal cortex.
(**a**) A representative cryo-EM images of α-synuclein filaments from the temporal cortex and the frontal cortex of an atypical MSA patient. Scale bar, 50 nm. (**b**) Two-dimensional class averages spanning an entire crossover of the Lewy-MSA hybrid filaments. Scale bar, 10 nm. Approximately 10% of the filaments from the frontal cortex exhibited a distinct two-dimensional class average from the Lewy-hybrid filaments which was suboptimal for structure determination.

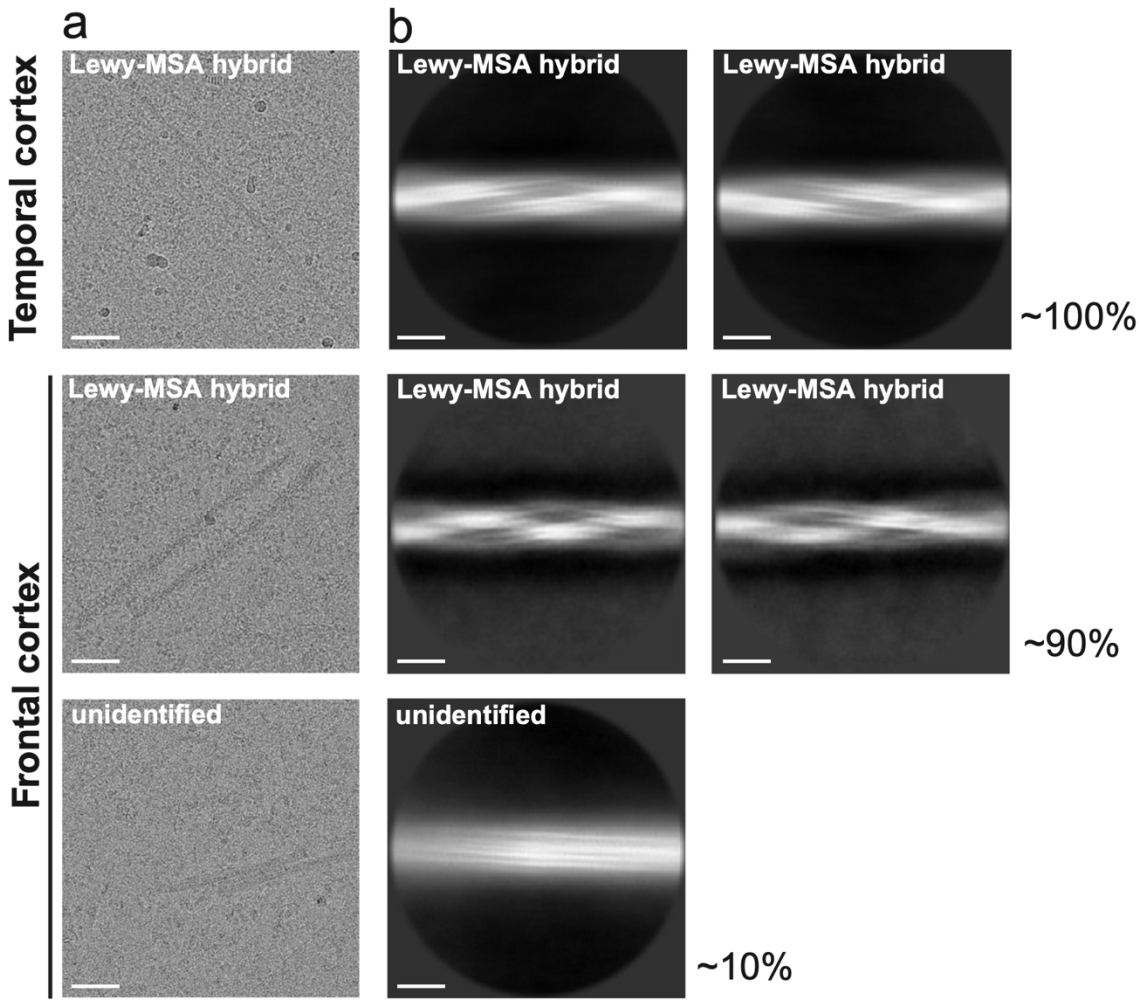

Suppl-Fig. 5. Cryo-EM maps and resolution evaluation of the refined models.
(**a, b**) Side view of the Lewy-MSA hybrid filaments from the temporal cortex (**a**) and the frontal cortex (**b**). Scale bar, 5 nm. (**c, d**) Fourier shell correlation (FSC) curve of two independently refined half-maps (black line); FSC curve of final cryo-EM reconstruction and refined atomic model (red); FSC curve of first half-map and the atomic model refined against this map (blue); FSC curve of second half-map and the atomic model refined against the first half-map (yellow dashes) of the filaments from the temporal cortex (**c**) or the frontal cortex (**d**). (**e, f**) The local resolution estimations of cryo-EM maps of Lewy-MSA hybrid/MSA doublet filaments from the temporal cortex (**e**) and the frontal cortex (**f**).

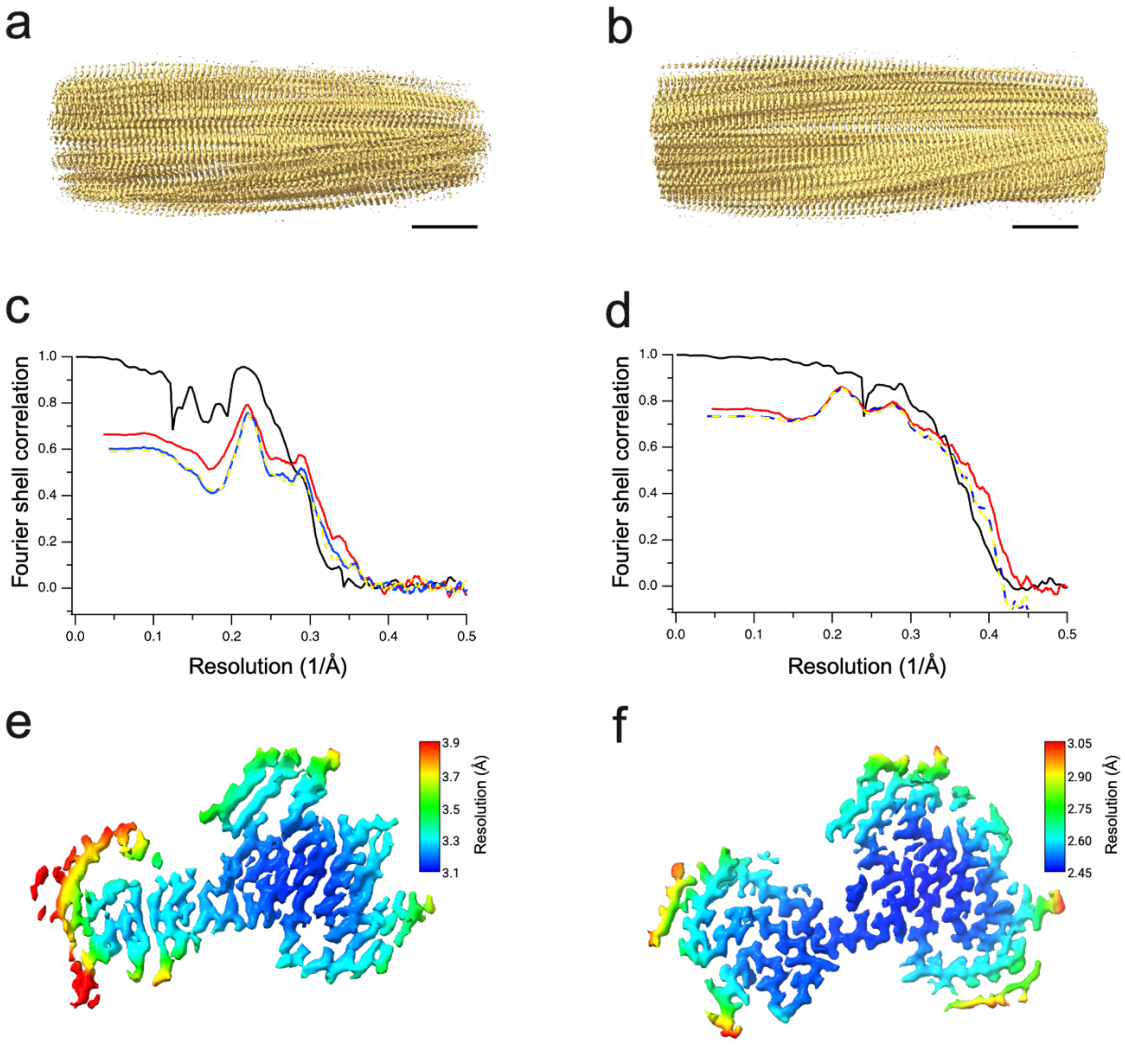

Suppl-Fig. 6. Comparison of the non-proteinaceous densities surrounded by the four lysines. (**a**) Superposition of Lewy-L (light blue) and the Lewy fold of LBD (magenta). (**b, c, d**) Comparison of the non-proteinaceous density of Lewy-L (light blue) with that of the Lewy fold of LBD (magenta) (**b**), MSA Type I (orange) (**c**) or MSA Type II (purple) (**d**). Structural alignments were performed using K32-K45 for the Lewy fold of LBD, K43-H50 for MSA Type I and II, respectively. The non-proteinaceous density for Lewy-L is colored with light blue and those for the Lewy fold of LBD and MSA Type I and II are colored with yellow.

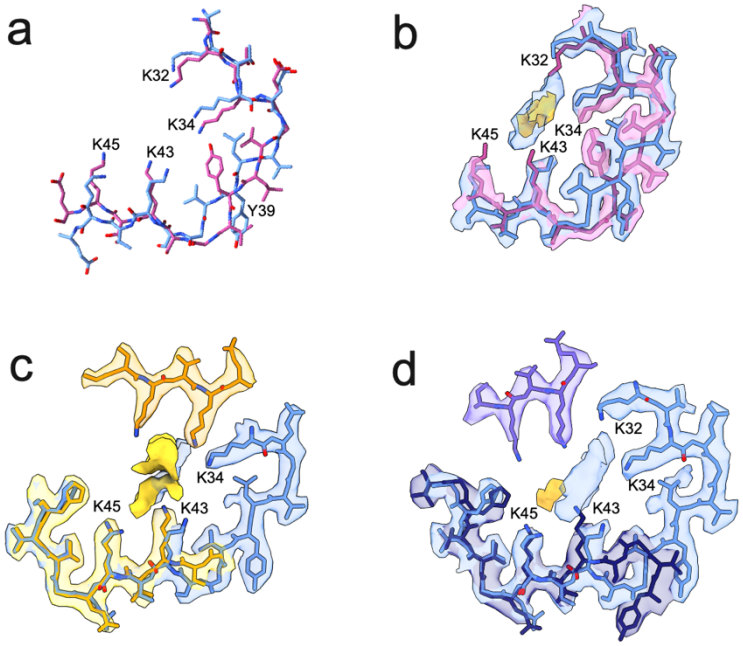

Suppl-Fig. 7. Screenshot of B allele frequency and LogR ratio plots for the case with atypical MSA in chromosome browser, genomestudio.